Three-Dimensional Kaleidoscopic Imaging

Ilya Reshetouski *
Saarland University

Alkhazur Manakov
Saarland University

Hans-Peter Seidel
MPI Informatik

Ivo Ihrke
Saarland University

Abstract

We introduce three-dimensional kaleidoscopic imaging, a promising alternative for recording multi-view imagery.

The main limitation of multi-view reconstruction techniques is the limited number of views that are available from multi-camera systems, especially for dynamic scenes.

Our new system is based on imaging an object inside a kaleidoscopic mirror system. We show that this approach can generate a large number of high-quality views well distributed over the hemisphere surrounding the object in a single shot. In comparison to existing multi-view systems, our method offers a number of advantages: it is possible to operate with a single camera, the individual views are perfectly synchronized, and they have the same radiometric and colorimetric properties.

We describe the setup both theoretically, and provide methods for a practical implementation. Enabling interfacing to standard multi-view algorithms for further processing is an important goal of our techniques.

1. Introduction

Since its invention by David Brewster in 1815 the Kaleidoscope has fascinated our minds. Its ability to generate hundreds of intricately interwoven views of the same object generates beautifully patterned images. For imaging purposes kaleidoscopic systems have so far been used for reflectance measurements [9, 1] owing to their ability to generate a large number of views of the target, almost covering the full hemisphere surrounding the measured surface patch.

The limitation of only being able to image planar objects is due to the fact that three-dimensional objects are not restricted to be imaged in simple regions in the camera view. It is a-priory impossible to determine the virtual view of any one pixel if the object geometry is unknown. A major challenge is potential self-occlusion of the object that is being imaged. The effect is familiar from viewing ones own image in-between a set of bathroom mirrors.

*iresheto@mmci.uni-saarland.de

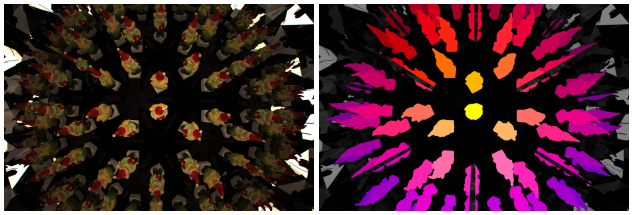

Figure 1. The pixel labeling problem solved by our algorithm: In a kaleidoscopic mirror system, objects occlude their mirror images (left). With unknown object geometry, it is a-priory impossible to determine the virtual view of any particular pixel. The techniques proposed in this paper determine a labeling, assigning a virtual view to every pixel (right, virtual views are color-coded).

In this paper, we propose a general solution to this problem, see Fig. 1.

So far, the occlusion problem has been circumvented by only using simple planar mirror systems for virtual multi-view imaging. Examples include the use of planar mirrors to generate virtual stereoscopic views [20, 6, 7] and virtual multi-view systems consisting of two planar mirrors arranged such that 5 or 7 object views can be obtained [4, 11, 14, 28]. When using these systems, however, care has to be taken to position the object such that there is no occlusion between the real object and its mirror images. Also, higher-order reflections (in this case not higher than two or three), should not overlap.

Another way to acquire multi-view imagery is the use of multi-camera systems [27] or light field camera designs [17, 8, 22]. These options are typically expensive if many cameras are used or involve time-sequential capture. In addition, available sensor resolution is used inefficiently, mostly recording background information. For in-camera light field imaging, e.g. [22], there is the limited aperture of the main lens and thus the achievable coverage of view-points is limited. Time sequential capture can also be performed with a moving planar mirror [21, 12, 10]. Mirrors have also been used to capture light field information [16, 24] but without considering inter-reflections. Light field imaging has also been performed with a conical mirror [25]. More typically, catadioptric systems are used to achieve a wide field of view as in panoramic imaging, e.g. [18]. 3D reconstruction using a conical mirror device

by taking multiple images has also been demonstrated [13].

In contrast to these techniques, we aim at performing massively multi-view imaging with a single high-resolution camera using only a single image. The virtual views should cover a large amount of viewing directions and the sensor area of the camera should be used as efficiently as possible. Kaleidoscopic imaging systems are a means to achieve this goal if the pixel labeling problem can be solved.

More precisely, we introduce techniques to determine which virtual view is associated with any one pixel in a kaleidoscopic image, see Fig. 1 (right). For this, we develop a theoretical framework that lets us describe arbitrary systems of planar mirrors that are being imaged by a projective camera.

We present calibration and processing techniques for kaleidoscopic imaging systems that enable an almost transparent interface to standard multi-view reconstruction techniques. The motivating factor is that existing algorithms should not be required to change if a new imaging modality becomes available.

For this reason, we do not assume any scene-dependent characteristics other than that foreground and background be separable, i.e. kaleidoscopic silhouette images should be available. We aim at labeling all silhouette pixels in a kaleidoscopic image according to the virtual view they belong to using only a single silhouette image and the geometric properties of the imaging system.

This sets the agenda for the remainder of the paper. In Sect. 2 we introduce a general framework to perform this labeling for any system consisting of planar mirrors and a projective camera. Sect. 3 then introduces a prototype system with which we verify our ideas. We also present suitable calibration procedures for such a system. In Sect. 4 we describe a number of experiments we performed to characterize our system. Sect. 5 then discusses the general properties and practical limitations of kaleidoscopic imaging devices before we conclude with a discussion of future work, Sect. 6.

2. Kaleidoscopic Imaging Theory

In mathematics, kaleidoscopic imaging systems have been analyzed in terms of group theory [3, 26]. In mathematical language, a kaleidoscopic system is one that, by repeated mirroring of a *base chamber*, Fig. 2 (a),

1. provides a perfect space-partitioning of the enclosing space, see Fig. 2 (b), and

2. maps the base chamber to virtual or mirror chambers in such a way that the orientation of the object it contains is preserved, irrespective of the sequence of mirror operations used to generate the mirror chamber, Fig. 2 (c).

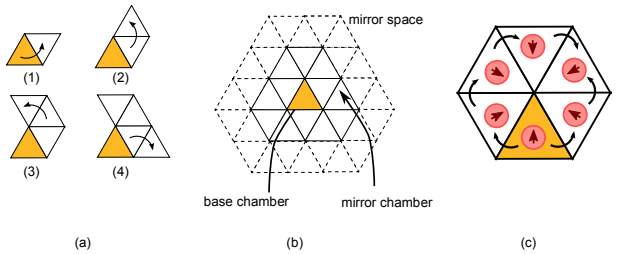

Figure 2. Mathematical kaleidoscopic systems generate a space partitioning by repeated mirroring of the base chamber (a). The partitioning covers the full space. We refer to it as mirror space (b). Additionally, mathematical kaleidoscopes are required to preserve the orientation of the mirrored chambers, irrespective of the mirroring sequence taken to generate the chamber (c).

If these two requirements are fulfilled the system generates a group of transformations where the basic transformations are defined by the mirrors of the base chamber and concatenation of transformations generates new members [3]. It should be noted that this construction is independent of any viewpoint for the scene. It is based on purely geometric considerations. The only kaleidoscopic structures in this sense are the rectangle, the equilateral triangle, the isosceles right triangle and the right triangles with $30°-60°-90°$ [3].

In this article, we interpret the term *kaleidoscopic* in a broader sense, using it to describe any system consisting of a number of planar mirrors in arbitrary configuration *in conjunction* with a projective imaging device such as a camera. We refer to such a system as a *generalized kaleidoscopic imaging system*. In the following we show that such a system also generates a space-partitioning but that it does not preserve the orientation of the chambers nor continuity between the chamber boundaries. For the purposes of three-dimensional imaging, however, these conditions are shown to be sufficient to allow for tractable and robust algorithms for the pixel labeling problem.

2.1. Space Partitioning

The goal of this subsection is to introduce the tools necessary to understand image formation in complex systems of planar mirrors. For convenience of illustration we develop the concepts in two dimensions, the generalization to the three-dimensional case is straight-forward. The value of a space-partitioning lies in the fact that every position in mirror space can be uniquely associated with a position in the base chamber, i.e. that there exists a surjective mapping between the mirror space and the base chamber.

Consider a pinhole camera with projective center C in the base chamber of a generalized kaleidoscopic imaging system. Our goal is to describe the resulting reflected ray geometry, see Fig. 3 (a), in an intuitive way.

The ray l is reflected off the mirrors and traverses them in a particular order $L_N = (3, 2, 1, 2, 1, 3, 1, \ldots)$ for a par-

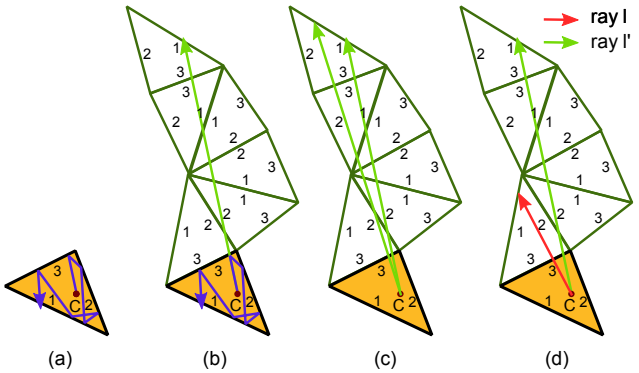

Figure 3. A ray in a generalized kaleidoscopic system is reflected off the planar mirrors (a). "Unfolding" of the ray can be performed by mirroring the base chamber instead of the ray (b). Two neighboring rays typically share a common unfolding scheme (c). Upon intersection with different mirror planes this coherence breaks down (d).

ticular number N of reflections. Here, L_N is an ordered N-tuple describing the mirror sequence that the ray intersects. It is indicative of the light path taken by the ray inside the system. We can "unfold" this light path by mirroring the base chamber instead of the ray, creating a sequence of mirror chambers along the straightened ray, see Fig. 3 (b). Upon transforming the mirror chambers, along with the ray segment contained therein, back to the base chamber, we re-obtain the "folded" light path of Fig. 3 (a).

In general, two neighboring light paths l and l', Fig. 3 (c), traverse the system in a similar manner, i.e. $L_N = L'_N$ for some reflection count N. This is the reason for obtaining recognizable virtual views in systems of planar mirrors. As long as this condition persists, the space partitioning generated by one of the rays, e.g. Fig. 3 (c), is a valid explanation for both l and l'. This argument breaks down when the two rays hit different mirrors at some reflection count $\hat{N} > N$, see Fig. 3 (d), and $L_{\hat{N}} \neq L'_{\hat{N}}$.

Let us investigate this case more closely. The situation is depicted in Fig. 4 (a). Two neighboring rays l and l' are incident on two different mirrors after having traversed the base chamber and two mirror chambers similarly, i.e. $L_2 = L'_2 = (2,1)$, but $L_3 = (2,1,3) \neq (2,1,2) = L'_3$. Unfolding the light paths in this case leads to a situation which is incompatible with a space-partitioning, Fig. 4 (b). Even though the rays can be extended to $L_4 = (2,1,3,2)$ and $L_4 = (2,1,2,3)'$, respectively, the next extension is uncertain. The overlapping mirror chambers offer two explanations for part of the mirror space.

The situation can be resolved, however, using the fact that rays l and l' share a common point, i.e. the center of projection C. In fact, all rays share this point. Using this information it is easy to see that a proper space partitioning can be obtained by using the chamber system generated by l

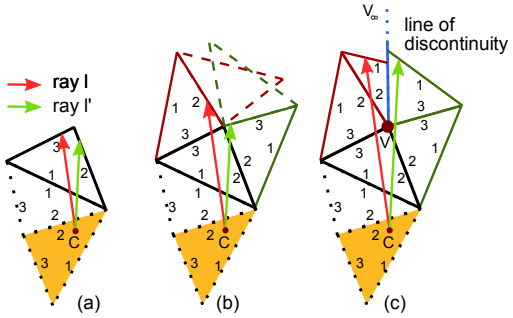

Figure 4. Two neighboring rays approaching an intersection with different mirror planes (a), the space partitioning is common for both rays so far. Propagating the rays further, a collision between space partitioning explanations occurs (b). It can be resolved by introducing a line of discontinuity (c).

to the left of the segment $[V, V_\infty)$, and the one generated by l' to its right. We call these *lines of discontinuity* referring to the discontinuity introduced into the mirror space. It is obvious that no other ray passing through C can intersect $[V, V_\infty)$ except for the one that is passing through C and V.

Summarizing, the space partitioning scheme provides us with a tool to unfold mirrored light paths, turning them into straight rays. The individual ray segments can then be folded back by transforming the containing (potentially partial) mirror chamber onto the base chamber. This way, any point in the virtual mirror space can be associated uniquely with a point in the base chamber (the opposite is not true). It should also be noted that every mirror chamber in mirror space corresponds to a unique camera view as seen from camera center C. In the following we are thus able to apply tools from projective reconstruction to our setup, namely the visual hull concept [15].

2.2. System Containing Objects

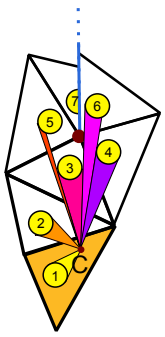

Ultimately, our goal is to label each pixel of our projective camera image with the mirror chamber where its corresponding ray intersects the object. As discussed before, this information corresponds to determining the virtual view point for each pixel of the kaleidoscopic view. An illustration of this is shown in the figure to the left. Differently colored cones encode different viewpoints of the object. The cutaway virtual object generated by the line of discontinuity is blocked by self-occlusion. Objects $1-4$ are fully visible, 5 and 6 are partially visible while 7 is fully occluded. Even if 7 was visible, only part of it could be observed due to the space partitioning introduced by the mirrors.

To achieve the labeling, it is necessary to infer some geometric structure of the object under consideration. As can

be seen from the figure, once the object geometry is known, labeling the pixels is trivial. The object only has to be rendered in all its visible mirrored positions, as determined by the space-partitioning of the system, with occlusion taken into account.

Our method to determine an approximate geometry of the object is based on considering rays that do *not intersect* any real or mirrored version of the object. However, if an unlimited number of reflections is permitted, an extended object is visible in *all* pixels [5]. It is thus necessary to limit the number of mirror reflections that can occur in a kaleidoscopic system.

2.2.1 Limiting the Number of Mirror Reflections

To limit the number of virtual views it is necessary to switch to the three-dimensional case. In three dimensions it is possible to adjust the tilt of the mirror planes such that any incident ray undergoes at most $N = \lceil \frac{\pi}{\alpha} \rceil$ reflections, where N only depends on the tilt angle [5].

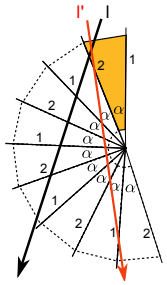

The figure to the left shows a two-dimensional cut-away view of a three-dimensional base chamber (yellow) with tilted mirrors. At the apex, the angle is α. Unfolding the base chamber to generate the mirror space, we immediately see that an arbitrary ray cannot cross more then $N + 1$ chambers (including the base chamber), i.e. the number of reflections is limited to N. The ray indicated in red is the limiting case of grazing incident angles at mirror 1.

2.2.2 Reconstructing the Visual Hull of the Object

With a limited number of virtual views it is possible to devise a setup where gaps between an object and its mirror images are observable. These gaps provide the means to perform a visual hull reconstruction of the object.

Consider a ray that does not intersect the object nor any of its virtual counterparts. Folding back this ray into the base chamber, we obtain a reflected light path that is guaranteed to be free of intersections. Performing this operation on the set of all rays that do not intersect the object anywhere in mirror space, we obtain a space carving scheme to determine the visual hull of the object: It is computed by successively removing free space from an initial volume that is marked as containing the object.

2.2.3 Labeling the Image

The visual hull computed this way can effectively be used as a geometric proxy for the object. By transforming the visual hull into the mirror chambers and intersecting the straightened camera rays in unfolded mirror space with the set of mirrored visual hulls, we can label the rays w.r.t. the mirror chamber where the ray first intersects the visual hull. This way a virtual view of the object is determined for each pixel.

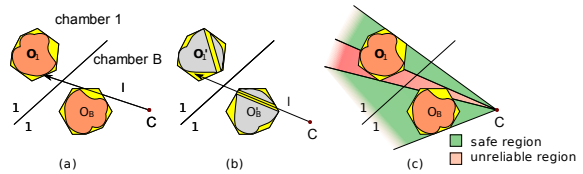

Figure 5. Unreliable pixel labeling can occur by a ray intersecting the approximate visual hull while the real ray passes the object. Two cases are important: (a) the ray passes at an object boundary and (b) the object has a hole that cannot be recovered from silhouette information. The pixels can be grouped into reliable and unreliable pixels according to the number of visual hulls they intersect (one and more than one respectively).

There is one important drawback to this scheme: the visual hull is not the true object geometry (in fact the visual hull as seen by an equivalent real camera system would be sufficient, but it is also unknown). Especially in cases of overlapping silhouettes it is possible that rays that intersect the visual hull do not actually intersect the real object, see Fig. 5.

In practical situations, the case of Fig. 5 (a) is the most important. The visual hull as obtained from the mirror system is slightly too large and the ray l is not intersecting object O_B while intersecting its approximate visual hull. The pixel is classified as belonging to base chamber B. In reality, however, the ray intersects the virtual object O_1 obtained by reflection through mirror 1 and thus should be labeled as belonging to chamber 1.

We have been unable to provide a narrow classification rule for these types of pixels. We can however show that the problem is unsolvable for general objects and that there is thus no simple solution, i.e. one without heuristics. Consider the case of Fig. 5 (b). The real object O'_B, which has the same approximate visual hull as O_B, has a very narrow hole (in the limit a Dirac-like opening only permitting a single ray), only visible from C. The ray passes through the hole but is blocked by virtual object O'_1. Since the hole direction only permits a single ray, the hole is not visible from any other direction. It is thus impossible to update the visual hull to include the hole and the labeling fails. The proper course of action is to classify all pixels corresponding to rays intersecting more than one real or virtual object as *unreliable* which means that they cannot be properly assigned to any particular view, see Fig. 5 (c). Note however that there is only a certain number of candidate views, namely the ones corresponding to the intersected virtual objects. Future multi-view algorithms could exploit this information.

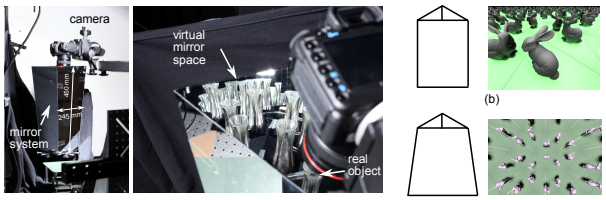

Figure 6. Photograph of our practical setup, (a) left. A view inside showing the mirror space, (a) right. (b) and (c): alternative setups and simulated images for these.

In practice the hole problem, Fig. 5 (b) is insignificant in all cases that we investigated. The case of Fig. 5 (a) however, where different virtual views meet side by side, is unavoidable except for simple systems where there is no overlap between mirror images. The better the visual hull approximation to the true visual hull, the smaller is this error. Since we have a large number of views (typically around 200 usable ones) this error is small and can be mitigated by enforcing a safety region around occlusion boundaries in image space.

3. Practical Implementation

It should be noted that the tools developed so far are applicable to any system of planar mirrors imaged by a projective camera. In the following we concentrate on a specific kaleidoscopic setup to verify our theoretical developments in practice.

3.1. Design Choices

We chose the frustum of a triangular pyramid as our base chamber, the narrow end pointed downward, see Fig. 6 (a). This type of system is preferable to the ones shown in Fig. 6 (b) and (c). In (b) the number of virtual views cannot be limited, yielding a cluttered horizon without usable gaps between the virtual views. In (c) we obtain views as if the camera was placed inside a giant sphere, the object being on the surface. In this type of setup the views can be separated but the object is always seen from the top, resulting in a low view point variation.

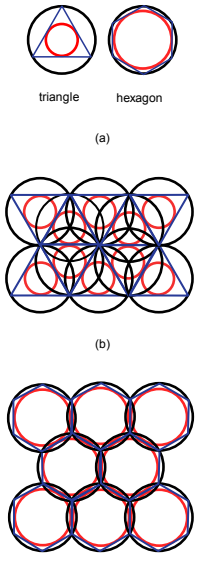

Figure 7.

The triangular base was chosen for both theoretical and practical reasons. The latter include simplicity of the system and its construction as well as simplified calibration procedures. On the theoretical side, the most important point to consider is the depth-of-field of the camera. Since we have to work with finite apertures, there is only a certain depth range where blur-free virtual views can be acquired. It is thus desirable to fit as many virtual views as possible into that range.

Consider a circular area being available for the base chamber, i.e. the black circle in Fig. 7 (a). The figure shows two different candidate base chamber geometries. Two copies of the base chamber can be placed next to each other at a distance the diameter of the inscribing red circle. The radius of the incircle is given by $r = R\cos\frac{\pi}{n}$, where R is the radius of the circumcircle and n the number of sides of the polygon. Clearly the ratio R/r should be as small as possible for fitting the most virtual views into a given depth range. This minimum is obtained for the triangle. A comparison of a triangular and a hexagonal space-partitioning scheme are shown in Figs. 7 (b) and (c).

We chose the opening angle of the system to permit up to 10 levels of reflection ($\approx 6.8°$). The setup was recorded by a Canon 5D Mark II equipped with a Canon EF14mm f/2.8L USM lens. The smallest aperture of this lens is $f/22$. We set it to $f/20$ for our experiments to limit diffraction effects. The mirrors are optical front-surface mirrors in the low end of the price range ($\approx$ \$200).

3.2. Geometric Calibration

We calibrate the intrinsic parameters of the camera using a number of checkerboard images using Zhang's method [29] as implemented in Bouguet's calibration toolbox [2]. We then place the camera into our setup and observe a checkerboard pattern placed in the kaleidoscope at different heights above the ground plane. This measure helps to keep the calibration consistent in the whole acquisition volume. We remove radial distortion from the images and identify the real image as well as the first-order reflections of the checkerboard. We compute plane equations using the known intrinsics and from those estimate initial guesses for the mirror planes. We perform a bundle adjustment procedure, optimizing the camera extrinsics and the mirror plane parameters while keeping the intrinsics fixed. We then use this initial calibration to predict the position of the second-order reflections. Matching to the extracted corners we optimize again to minimize the reprojection error. We then proceed in a similar manner to add third- and higher-order reflections. The checkerboards are typically well visible up to the sixth reflection order and we use all of this information in a final bundle adjustment of all parameters, camera intrinsics, extrinsics and mirror plane parameters. The reprojection error is typically within 1.2 pixels.

3.3. Radiometric Calibration

We first linearize the camera response by taking exposure sequences of 5 images and applying the technique of Robertson et al. [23] as implemented in the PFSTools package [19]. We then perform high-dynamic range imaging of a Spectralon target, an almost perfectly Lambertian reflector, under illumination generated by placing an area light source close to the kaleidoscope's upper opening. Since the light source is mirrored in the same manner as the view point, we obtain a uniform incident light distribution on the Spectralon patch. The patch should thus appear uniform under different viewing directions. However, since our virtual views are generated by mirroring rays, the images are attenuated by the mirror surface. To estimate the attenuation factor, we extract image patches of the Spectralon target for virtual views with different reflection counts and compute the median color value of the patch. Ratios of values from viewpoints of different reflection count then allow for the estimation of the attenuation coefficient. Using this procedure, our mirrors were estimated to have 87% reflectivity, this value being in good agreement for all color channels.

3.4. Space Carving Implementation

We implemented our space carving scheme as a voxel-based algorithm. The voxel grid is defined in the base chamber. To account for diverging rays we implemented a subsampling scheme for the pixels in the camera view. We also exclude a region of $\epsilon \approx 5$mm around the planes of discontinuity to avoid erroneous ray paths due to potential errors in the estimation of the mirror plane parameters. To achieve the most efficient use of the available resolution, the size of the bounding box of the voxel grid is chosen to enclose the object tightly. The number N of reflection levels to be used for visual hull reconstruction and pixel labeling is a user parameter to our algorithm.

4. Experimental Results

We recorded our images at a resolution of 3866×2574 pixels. The data sets as well as the computed labeling and radiometrically corrected images are shown in Fig. 8. Table 1 summarizes some statistics. All results have been computed only using the silhouette image shown in Fig. 8 and the calibration information. The objects cover different sizes and vary drastically in silhouette quality. The results have been down-sampled for the paper due to size restrictions, please refer to the supplemental material for higher-resolution results. The results in the figure were computed using the information from 8 levels of reflection, equalling 166 views. For 9 reflection levels results deteriorated due to insufficient accuracy of the silhouette estimation (chromatic aberration) and residual radial distortion, see Sect. 5. The dark streaks in the images are due to the safety region around mirror boundaries. As can be seen in the results, we achieve almost pixel-accurate labeling results: if errors occur, they are conservative, i.e. to the inside of the object, the labeling is thus still correct. Overlaps between virtual views can be well resolved. The table shows that the unreliable pixel measure is overly conservative and that a heuristic can yield a much higher usable pixel count. Since the objects do not have narrow holes this approach appears reasonable. Further results can be found on our web page: http://giana.mmci.uni-saarland.de/projects/kaleidoscopic_imaging/.

5. Discussion

In this section we would like to discuss the physical limitations of kaleidoscopic imaging systems as well as general properties of the proposed algorithm.

We are operating the camera at the physical limits of the optics. The most important aspect is the limited depth-of-field of real camera systems. Since the virtual views cover a very wide depth range, both very close to the camera for the imaged real object and very far away, for the distant reflections, a suitable trade-off has to be found. Also, we use a very wide field-of-view to cover the planet structure imposed by our prototype system. This implies that the higher-order reflections which carry a lot of silhouette information, since the object is seen from the side in these views, are imaged at the periphery of the image. Thus, any uncorrected radial distortion and in particular other optical aberrations found in these regions are of major concern. Chromatic aberration was a major problem in our experiments. The correct silhouette boundary is not discernible even by a human observer. The spread of the aberration is up to 7 pixels, a much higher value than the geometric calibration error. Use of a different lens might reduce this problem.

Incorrect silhouettes should never under-estimate the object since this would lead to erroneous space carving results. Surprisingly coarse silhouette estimates can in fact be used with such system, see Fig. 8. The condition is that the inaccuracies should not be correlated. Since a very high number of views is available, geometric inconsistencies tend to be discovered. However, a consistent over-estimation of the silhouettes introduces errors.

An inherent property of our data is that they are multi-resolution. Pixels in distant images of higher reflection levels cover a larger surface area of the object. This apparent disadvantage might turn out to be a useful feature in future multi-view reconstruction algorithms. In any case it is a particular property that cannot be achieved easily in different systems.

Finally, scaling of the setup might present a problem. However, e.g. Science World in Vancouver is operating a kaleidoscope at human proportions. Foil mirrors can easily be produced up to a size of $4 - 5$m. We thus believe that

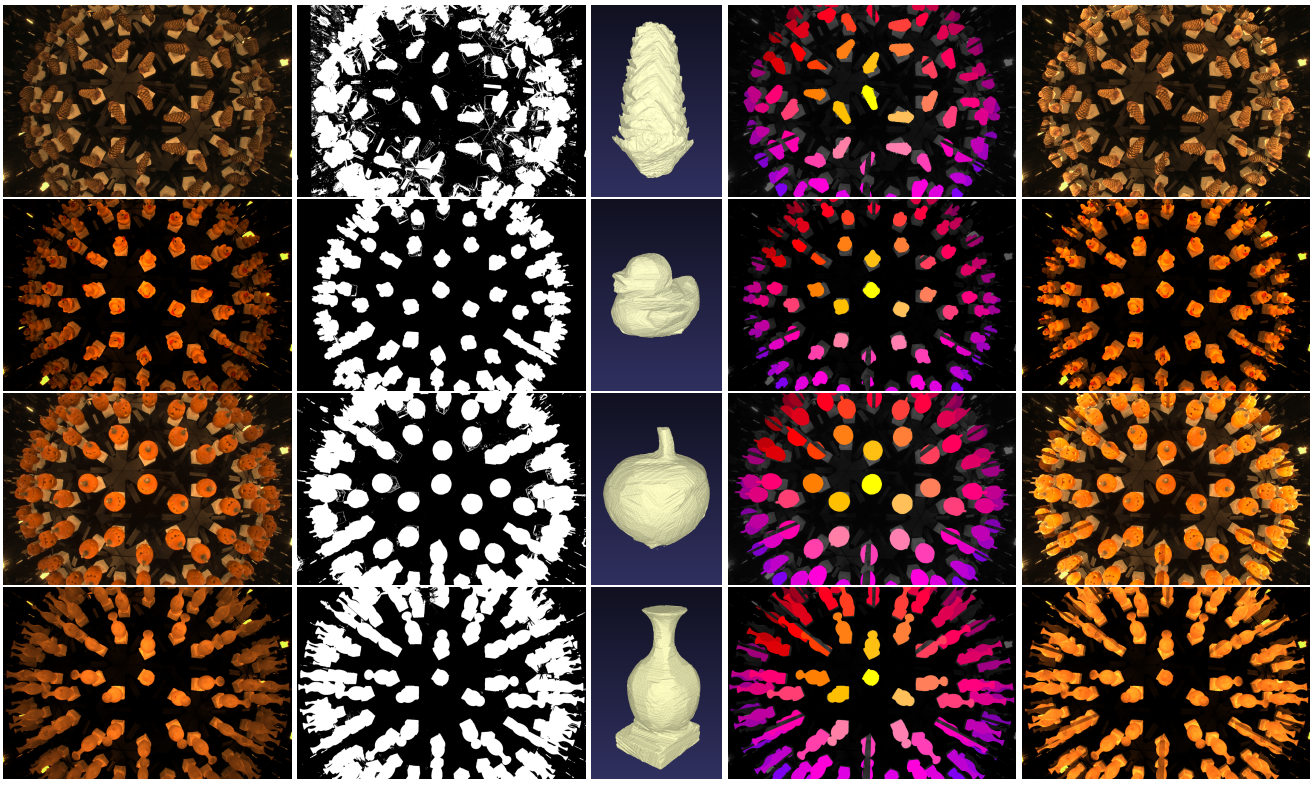

Figure 8. Results from left to right: input image, silhouette image, computed visual hull, corresponding labeling, radiometrically compensated image.

object	# refl.	subsample	VH disc.	# virt. views	# labeled pixels	# unreliable	# occ. boundary
Cone	7	9	$256 \times 256 \times 236$	128	18.38%	2.31%	0.08%
Cone	8	9	$256 \times 256 \times 236$	166	19.60%	4.44%	0.12%
Cone	9	9	$256 \times 256 \times 236$	212	19.91%	5.04%	0.20%
Duck	7	9	$256 \times 256 \times 221$	128	15.16%	1.44%	0.06%
Duck	8	9	$256 \times 256 \times 221$	166	15.94%	3.46%	0.12%
Duck	9	9	$256 \times 256 \times 221$	212	16.24%	5.97%	0.19%
Pumpkin	7	9	$300 \times 300 \times 346$	128	25.70%	5.89%	0.16%
Pumpkin	8	9	$300 \times 300 \times 346$	166	27.20%	8.94%	0.21%
Pumpkin	9	9	$300 \times 300 \times 346$	212	27.79%	12.86%	0.26%
Vase	7	9	$256 \times 256 \times 354$	128	29.02%	10.64%	0.25%
Vase	8	9	$256 \times 256 \times 354$	166	30.41%	13.49%	0.33%
Vase	9	9	$256 \times 256 \times 354$	212	31.08%	15.29%	0.39%

Table 1. Statistics for the different data sets. From left to right: name of the data set, number of reflection levels used to compute result, number of sub-samples per pixel, discretization of the visual hull, number of virtual views that have been used for computation, the number of labeled pixels, unreliable pixels as a percentage of labeled pixels, and number of pixels in a 3 pixel error region to each side of an occlusion boundary.

these systems are applicable to real problems of interest.

6. Conclusions and Future Work

We have introduced a general framework for dealing with systems of planar mirrors imaged by a projective camera. We have shown that these generalized kaleidoscopic imaging systems can be used to obtain dense hemispherical multi-view data that is calibrated both geometrically and photometrically. The output of our techniques is thus directly usable in standard multi-view reconstruction algorithms. All information can be extracted from a single view, enabling dynamic scene recording. We thus believe that the proposed methods present a considerable step towards high quality 3D reconstruction of dynamic objects, enabling

practical hemispherical imaging. Due to the wide range of views achievable with these systems it is possible to image every surface point from a large number of directions. It might thus become possible to perform simultaneous geometry and reflectance estimation on dynamic objects. The setup is inexpensive when compared to multi-video acquisition systems and makes better use of the available sensor area. Additional advantages include perfect synchronization and common radiometric and colorimetric properties for all views.

Future work includes the development of better calibration procedures. It might be necessary to develop better camera models for this purpose since we are operating at the physical limits of our device, especially the optics. On the theoretical side we would like to develop rigorous bounds for the pixel labeling error at occlusion boundaries. Since this is impossible in the general case, suitable object classes that cover all scenes of interest while still enabling an estimation of a tight error bound have to be found. Future algorithmic developments include the incorporation of inherently multi-resolution data in multi-view reconstruction algorithms as well as investigating techniques to differentiate between the limited number of views that are potentially responsible for unreliable pixels.

Acknowledgements

This work was funded by the German Research Foundation (DFG) within the Cluster of Excellence “Multimodal Computing and Interaction”.

References

[1] S. Bangay and J. D. Radloff. Kaleidoscope Configurations for Reflectance Measurement. In *Proc. AFRIGRAPH*, pages 161–170, 2004. 353

[2] J.-Y. Bouguet. Camera Calibration Toolbox for Matlab, 2005. 357

[3] H. S. M. Coxeter. Discrete Groups Generated by Reflections. *The Annals of Mathematics*, 35(3):588–621, July 1934. 354

[4] K. Forbes, F. Nicolls, G. D. Jager, and A. Voigt. Shape-from-Silhouette with two Mirrors and an Uncalibrated Camera. In *Proc. ECCV*, pages 165–178, 2006. 353

[5] G. A. Galperin and A. N. Zemlyakov. Mathematical Billards (in Russian). *Kvant*, 77, 1990. 356

[6] J. Gluckman and S. K. Nayar. Planar Catadioptric Stereo: Geometry and Calibration. In *Proc. CVPR*, page 1022, 1999. 353

[7] J. Gluckman and S. K. Nayar. Rectified Catadioptric Stereo Sensors. In *Proc. CVPR*, page 2380, 2000. 353

[8] S. Gortler, R. Grzeszczuk, R. Szelinski, and M. Cohen. The Lumigraph. In *Proc. SIGGRAPH*, pages 43–54, 1996. 353

[9] J. Y. Han and K. Perlin. Measuring Bidirectional Texture Reflectance with a Kaleidoscope. In *Proc. SIGGRAPH*, pages 741–748, New York, NY, USA, 2003. ACM. 353

[10] B. Hu. It’s All Done with Mirrors: Calibration-and-Correspondence-Free 3D Reconstruction. In *Proc. CRV*, pages 148–154, 2009. 353

[11] P.-H. Huang and S.-H. Lai. Contour-Based Structure from Reflection. In *Proc. CVPR*, pages 165–178, 2006. 353

[12] I. Ihrke, T. Stich, H. Gottschlich, M. Magnor, and H.-P. Seidel. Fast Incident Light Field Acquisition and Rendering. *Journal of WSCG*, 16(1-3):25–32, 2008. 353

[13] S. Kuthirummal and S. K. Nayar. Multiview Radial Catadioptric Imaging for Scene Capture. *ACM Trans. Graph.*, 25(3):916–923, 2006. 354

[14] D. Lanman, D. Crispell, and G. Taubin. Surround Structured Lighting: 3-D Scanning with Orthographic Illumination. *Computer Vision and Image Understanding*, (113):1107–1117, 2009. 353

[15] A. Laurentini. The Visual Hull Concept for Silhouette-Based Image Understanding. *IEEE Trans. PAMI*, pages 150–162, 1994. 355

[16] M. Levoy, B. Chen, V. Vaish, M. Horowitz, I. McDowall, and M. Bolas. Synthetic aperture confocal imaging. *ACM Trans. Graph.*, 23:825–834, August 2004. 353

[17] M. Levoy and P. Hanrahan. Light Field Rendering. In *Proc. SIGGRAPH*, pages 31–42, 1996. 353

[18] S.-S. Lin and R. Bajcsy. 3-D Reconstruction Using Mirror Images Based on a Plane Symmetry Recovering Method. *IEEE Trans. PAMI*, 28:840–845, May 2006. 353

[19] R. Mantiuk. PFSCalibration, 2006. 358

[20] H. Mitsumoto, S. Tamura, K. Okazaki, N. Kajimi, and Y. Fukui. 3-D Reconstruction Using Mirror Images Based on a Plane Symmetry Recovering Method. *IEEE Trans. PAMI*, 14:941–946, September 1992. 353

[21] D. W. Murray. Recovering Range using Virtual Multi-Camera Stereo. *Computer Vision and Image Understanding*, 61(2):285–291, Mar. 1995. 353

[22] R. Ng, M. Levoy, M. Brédif, G. Duval, M. Horowitz, and P. Hanrahan. Light Field Photography with a Hand-Held Plenoptic Camera. Technical Report Computer Science CSTR 2005-02, Stanford University, 2005. 353

[23] M. A. Robertson, S. Borman, and R. L. Stevenson. Estimation-Theoretic Approach to Dynamic Range Enhancement using Mutliple Exposures. *SPIE Journal of Electronic Imaging*, 12(2):219–228, April 2003. 358

[24] P. Sen, B. Chen, G. Garg, S. R. Marschner, M. Horowitz, M. Levoy, and H. P. A. Lensch. Dual photography. *ACM Trans. Graph.*, 24:745–755, July 2005. 353

[25] Y. Taguchi, A. Agrawal, S. Ramalingam, and A. Veeraraghavan. Axial Light Field for Curved Mirrors: Reflect Your Perspective, Widen Your View. In *Proc. CVPR*, pages 1–8, 2010. 353

[26] È. B. Vinberg. Discrete Linear Groups Generated by Reflections (in Russian). *Math. USSR Izvestija*, 5(5):1083–1119, 1971. 354

[27] B. Wilburn, N. Joshi, V. Vaish, E.-V. Talvala, E. Antunez, A. Barth, A. Adams, M. Horowitz, and M. Levoy. High Performance Imaging using Large Camera Arrays. *ACM Trans. Graph.*, 24(3):765–776, 2005. 353

[28] X. Ying, K. Peng, R. Ren, and H. Zha. Geometric Properties of Multiple Reflections in Catadioptric Camera with Two Planar Mirrors. In *Proc. CVPR*, pages 1 – 8, 2010. 353

[29] Z. Zhang. Flexible Camera Calibration By Viewing a Plane From Unknown Orientations. In *Proc. ICCV*, pages 666–673, Sept 1999. 357